Title

Limited Colonization Undermined by Inadequate Early Immune Responses Defines the Dynamics of Decidual Listeriosis

Journal

Infection and Immunity, 85(8)

ISSN

0019-9567

Authors

Rizzuto, Gabrielle
Tagliani, Elisa
Manandhar, Priyanka
et al.

Publication Date

2017-08-01

DOI

10.1128/iai.00153-17

Peer reviewed

AMERICAN SOCIETY FOR MICROBIOLOGY | Infection and Immunity®

CELLULAR MICROBIOLOGY:
PATHOGEN-HOST CELL MOLECULAR INTERACTIONS

Limited Colonization Undermined by Inadequate Early Immune Responses Defines the Dynamics of Decidual Listeriosis

Gabrielle Rizzuto,[a,b] Elisa Tagliani,[c] Priyanka Manandhar,[d,e] Adrian Erlebacher,[b,c,e*] Anna I. Bakardjiev[a,b]

Benioff Children's Hospital and Program in Microbial Pathogenesis and Host Defense, University of California—San Francisco, San Francisco, California, USA[a]; Biomedical Sciences Program, University of California—San Francisco, San Francisco, California, USA[b]; Department of Pathology, NYU School of Medicine, New York, New York, USA[c]; Department of Laboratory Medicine, University of California—San Francisco, San Francisco, California, USA[d]; Immunology Program, University of California—San Francisco, San Francisco, California, USA[e]

ABSTRACT The bacterial pathogen *Listeria monocytogenes* causes foodborne systemic disease in pregnant women, which can lead to preterm labor, stillbirth, or severe neonatal disease. Colonization of the maternal decidua appears to be an initial step in the maternal component of the disease as well as bacterial transmission to the placenta and fetus. Host-pathogen interactions in the decidua during this early stage of infection remain poorly understood. Here, we assessed the dynamics of *L. monocytogenes* infection in primary human decidual organ cultures and in the murine decidua *in vivo*. A high inoculum was necessary to infect both human and mouse deciduas, and the data support the existence of a barrier to initial colonization of the murine decidua. If successful, however, colonization in both species was followed by significant bacterial expansion associated with an inability of the decidua to mount appropriate innate cellular immune responses. The innate immune deficits included the failure of bacterial foci to attract macrophages and NK cells, cell types known to be important for early defenses against *L. monocytogenes* in the spleen, as well as a decrease in the tissue density of inflammatory Ly6C^{hi} monocytes *in vivo*. These results suggest that the infectivity of the decidua is not the result of an enhanced recruitment of *L. monocytogenes* to the gestational uterus but rather is due to compromised local innate cellular immune responses.

KEYWORDS *Listeria monocytogenes*, decidua, placenta

Received 25 February 2017 **Returned for modification** 25 March 2017 **Accepted** 8 May 2017

Accepted manuscript posted online 15 May 2017

Citation Rizzuto G, Tagliani E, Manandhar P, Erlebacher A, Bakardjiev AI. 2017. Limited colonization undermined by inadequate early immune responses defines the dynamics of decidual listeriosis. Infect Immun 85:e00153-17. https://doi.org/10.1128/IAI.00153-17.

Editor Nancy E. Freitag, University of Illinois at Chicago

Address correspondence to Anna I. Bakardjiev, Anna.Bakardjiev@ucsf.edu.

* Present address: Adrian Erlebacher, Department of Laboratory Medicine, University of California—San Francisco, San Francisco, California, USA.

The pregnant uterus is a dynamic organ that supports fetoplacental growth, with many trophic functions provided by the decidua, the specialized endometrial tissue that encases the conceptus (1). The decidua also provides a unique immunological environment that blocks the maternal immune system from recognizing the conceptus as a foreign tissue and rejecting it as if it were a solid-organ transplant (2). As a consequence, this environment would be expected to provide opportunities for pathogens to infect the maternal-fetal interface. Indeed, infection of the decidua is now considered to be a critical first step in the hematogenous transmission of a variety of pathogens from mother to fetus (3–7). One such organism is the facultative, intracellular, Gram-positive bacterium *Listeria monocytogenes*, a clinically relevant foodborne pathogen that can cause severe disease in pregnant women. Once *L. monocytogenes* reaches the placenta, there are increased risks of severe maternal disease and pregnancy complications, including preterm labor and devastating fetal/neonatal morbidity and mortality (8, 9).

Because of its experimental tractability, *L. monocytogenes* is an excellent model

organism to study host-pathogen interactions. The innate and adaptive immune responses to *L. monocytogenes* in murine liver and spleen have been an area of extensive study (reviewed in references 10 and 11) and reveal that innate responses prevent overwhelming bacterial growth at the early stages of infection, well before an adaptive response is generated. Classic studies by North and colleagues demonstrated that myeloid-lineage cells provide early defense against *L. monocytogenes*, since the absence of these cells transforms an otherwise sublethal intravenous inoculum to an overwhelming bacterial burden and leads to the death of infected animals within several days (12–14). More recent work identified dendritic cells (DCs) as the earliest-infected population and illustrated the rapid aggregation and swarming of neutrophils and monocytes at bacterial foci in the spleen (15, 16). Although tissue-resident macrophages, particularly liver Kupffer cells, likely contribute to early containment through their ability to produce free radicals via NADPH oxidase and inducible nitric oxide synthase (iNOS) (17), Ly6C^{hi} monocytes (Mos) are particularly indispensable for the early containment of *L. monocytogenes* in spleen and liver (18). Following monocyte chemoattractant protein 1 (MCP-1)- and MCP-3-mediated recruitment from the bone marrow (19, 20), CCR2^{+} Ly6C^{hi} Mos are activated *in situ* to differentiate into tumor necrosis factor alpha (TNF-α)/iNOS-producing DCs (Tip-DCs) (18, 21). Indeed, CCR2-deficient mice cannot eliminate splenic and hepatic *L. monocytogenes* bacteria (22). Thus, only if the bacterium has been sufficiently contained by this coordinated effort of macrophages, NK cells, and Ly6C^{hi} Mos/Tip-DCs in the first few days of infection are the ensuing adaptive responses able to ultimately clear the infection.

In contrast to murine liver and spleen, immunological mechanisms that might control *L. monocytogenes* at very early stages of decidual infection have not been subject to detailed characterization. The early stage of the host response in the decidua is particularly important because preexisting maternal adaptive T cell immunity does not protect the maternal-fetal interface from infection with *L. monocytogenes* (23). Interestingly, pregnant CSF-1 mutant *op/op* mice, which lack macrophages, and artificially decidualized macrophage-depleted mice show increased *L. monocytogenes* burdens within the placenta and uterus at 2 to 3 days postinfection, raising the possibility that macrophages control *L. monocytogenes* within the pregnant uterus (24). However, given that *L. monocytogenes* traffics from the maternal spleen and liver to the uterus (25), these results may be secondary to increases in the splenic or hepatic listerial burden. Furthermore, it is possible that macrophages in those experiments were responsible for local control within the placental tissue or myometrium but not the decidua *per se*, as the bacterial burden in isolated decidual tissue was not separately determined.

Indeed, descriptive work predicts that the decidua might be severely impaired in its ability to contain early infection by *L. monocytogenes*. For example, macrophages are relatively scarce within the murine decidua, while Ly6C^{hi} Mos do not enter this tissue under normal conditions despite being an abundant population attached to the decidual endothelium (26, 27). Furthermore, histological analysis of infected pregnant mice revealed a lack of macrophage colocalization with *L. monocytogenes* organisms within the antimesometrial decidua of implantation sites (6). When directly compared to the nonpregnant uterus, artificial deciduomas, which do not have fetoplacental units, also showed a lack of macrophage colocalization with *L. monocytogenes* in the antimesometrial decidua (28).

Here, we delineate very early immunological events during decidual infection with *L. monocytogenes*. Our data show that *L. monocytogenes* can grow in primary human decidual organ cultures but not primary human endometrial organ cultures and that there is an absence of macrophage colocalization with bacteria in the decidua. Using the artificial deciduoma and pregnant mouse models of infection, we show that specific aspects of the innate immune response are compromised in the decidua but are intact in the myometrium. Surprisingly, however, there was a restricted access of *L. monocytogenes* to both mouse and human deciduas, suggesting that the main defense against decidual infection may be at the level of initial seeding.

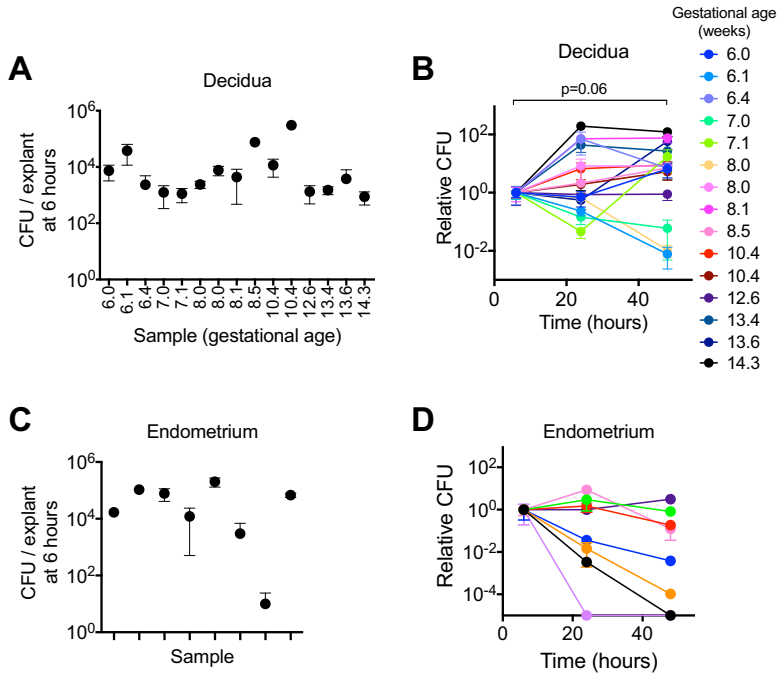

FIG 1 Infection of primary human decidual and endometrial organ cultures. Human decidual organ cultures from 15 donors (at least 3 cultures per donor at each time point) or endometrial organ cultures from 8 donors (1 to 3 cultures per donor at each time point) were incubated with 2×10^7 *L. monocytogenes* bacteria for 5 h prior to the addition of gentamicin. (A) Average CFU ± standard errors of the means of decidual organ cultures at 6 hpi. (B) Growth curve of the bacterial burden over time for each decidual donor ($n = 15$). Average CFU ± standard errors of the means for each donor at 24 and 48 hpi were normalized to data for the 6-h time point ($P = 0.065$ by ANOVA with repeated measures). Additionally, data were analyzed with Dunnett's multiple-comparison test to compare the relative CFU at 24 versus 6 hpi ($P = 0.13$) and at 48 versus 6 hpi ($P = 0.06$). (C) Average CFU ± standard errors of the means of endometrial organ cultures from each donor at 6 hpi. (D) Growth curve of the bacterial burden over time for each endometrial donor ($n = 8$). Average CFU ± standard errors of the means for each donor at 24 and 48 hpi were normalized to data for the 6-h time point ($P = 0.38$ by ANOVA with repeated measures). Additionally, data were analyzed with Dunnett's multiple-comparison test to compare the relative CFU at 24 versus 6 hpi ($P = 0.70$) and at 48 versus 6 hpi ($P = 0.41$).

RESULTS

Human decidua but not endometrium supports growth of *L. monocytogenes*. We studied *L. monocytogenes* infection of the human decidua using primary human organ cultures from decidual specimens ranging in gestational age from 6.0 to 14.3 weeks. Organ cultures were infected by incubation with 2×10^7 CFU of *L. monocytogenes* for 5 h, followed by the addition of gentamicin to the culture medium to kill extracellular bacteria. At 6 h postinfection (hpi), the median bacterial burden in decidual organ cultures was 3.8×10^3 CFU (range, 8.7×10^2 to 3×10^6 CFU/organ culture; $n = 15$) (Fig. 1A), indicating that only ~0.02% of the inoculum was able to invade decidual cultures. Subsequently, *L. monocytogenes* grew well in the decidua: the median fold increase in CFU was 7-fold (range, 0.008- to 122-fold) at between 6 and 48 hpi ($P = 0.06$) (Fig. 1B). Not uncommon when working with primary human tissues, there was strong variability in the bacterial burdens between tissues from different donors. In the majority of decidual specimens (73%; 11/15), numbers of bacteria increased at between 6 and 48 hpi by 2- to 200-fold, and the bacterial burdens were unchanged in tissue from one donor and decreased by <0.06-fold (range, 0.008- to 0.06-fold) in tissues from 20% (3/15) of donors (see Fig. S1A in the supplemental material). We observed a weak but significant correlation between the bacterial burden in the decidua and gestational age ($r^2 = 0.305$; $P < 0.05$) (Fig. S1B).

To determine whether the course of infection in the decidua differs from that in the nonpregnant endometrium, we established primary human endometrial organ cultures from benign hysterectomy specimens. The median bacterial burden at 6 hpi in endo-

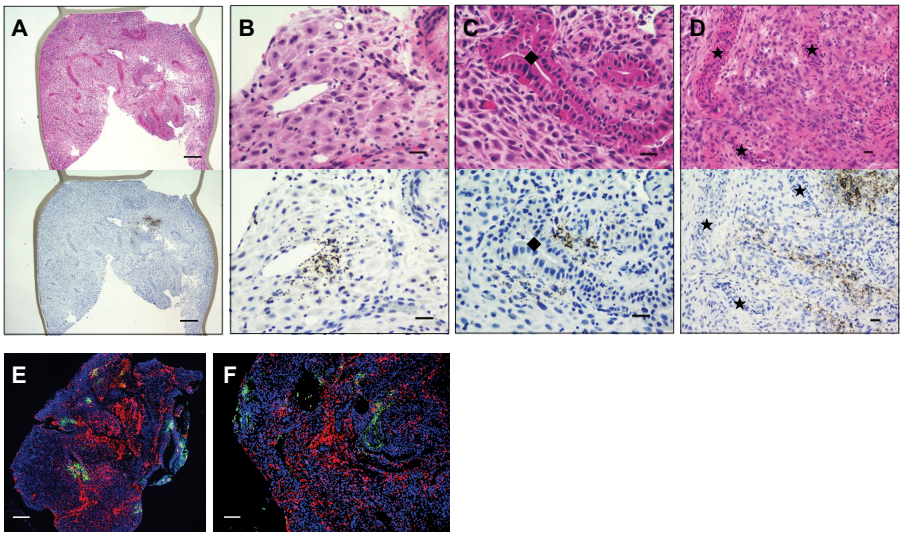

FIG 2 Infectious *L. monocytogenes* foci in the stroma of human decidual organ cultures. (A to D) Representative H&E-stained sections (top) and anti-*L. monocytogenes* IHC-stained sections (bottom) of infected decidual organ cultures at 24 hpi (A to C) and 72 hpi (D). Symbols label glands (◆) and vasculature (★) embedded in decidual stroma. Bars, 250 μm (A) and 25 μm (B to D). (E and F) Representative immunofluorescence microscopic images of infected decidual organ cultures at 72 hpi showing the distribution of CD68$^+$ cells (red) and *L. monocytogenes* (green). Bars, 250 μm (E) and 100 μm (F).

metrial organ cultures from 8 donors was 4.2×10^4 CFU, which correlates with 0.2% of the inoculum (range, 3.8×10^3 to 2×10^6 CFU in 7 donors and 1 outlier with only 10 CFU) (Fig. 1C). *L. monocytogenes* was unable to grow in the endometrium: the median CFU in endometrial cultures decreased by 15.7-fold at between 6 and 48 hpi (Fig. 1D).

We next subjected infected decidual organ cultures to histological analysis. These cultures showed typical decidual tissue architecture by hematoxylin and eosin (H&E) staining, with epithelium-lined glands and endothelium-lined vasculature embedded in decidualized stroma containing scattered immune cells (Fig. 2A, top). Immunohistochemistry (IHC) for *L. monocytogenes* revealed organisms predominantly in stromal cells in the vicinity of the vasculature at 24 hpi (Fig. 2A to C), progressing to larger zones of infected stromal regions at 72 hpi (Fig. 2D). Immunofluorescence staining for CD68$^+$ macrophages and *L. monocytogenes* revealed that macrophages did not accumulate around bacterial foci (representative images are shown in Fig. 2E and F). Similar microscopic studies could not be performed on endometrial specimens due to limited tissue availability. Thus, we cannot determine whether the decreased bacterial burden in endometrial cultures was correlated with a certain inflammatory cell pattern or a loss of host cell viability. Nonetheless, these results raised the possibility that macrophages might be unable to migrate to sites of *L. monocytogenes* infection within the human decidua, as was previously reported for the murine decidua (29).

The decidua is a barrier to infection *in vivo*. We next turned to mouse models to study decidual infection *in vivo*. Our previous demonstration that placental listeriosis involves a bottleneck to infection within the pregnant uterus (25) left open the question of whether the decidua itself limited *L. monocytogenes* infection. We therefore infected mice bearing artificial deciduomas to eliminate the confounding effects of fetal cells and tissues. Artificial deciduomas are masses of decidual tissue that form when an artificial stimulus, such as needle scratching or oil, is applied to the endometrium in a hormonally primed female (30). Importantly, deciduomas display biochemical, architectural, and immunological properties similar to those of true deciduas induced by the implantation of blastocysts (31, 32). We used a common approach to generate deciduomas, namely, mating female mice with vasectomized males, followed 3 days later (day 3.5 postcopulation [DPC3.5]) by intrauterine injection of sesame oil.

In our first set of experiments, we intravenously infected decidualized mice with a bioluminescent wild-type *L. monocytogenes* strain called 2C (33) on DPC6.5. *Ex vivo*

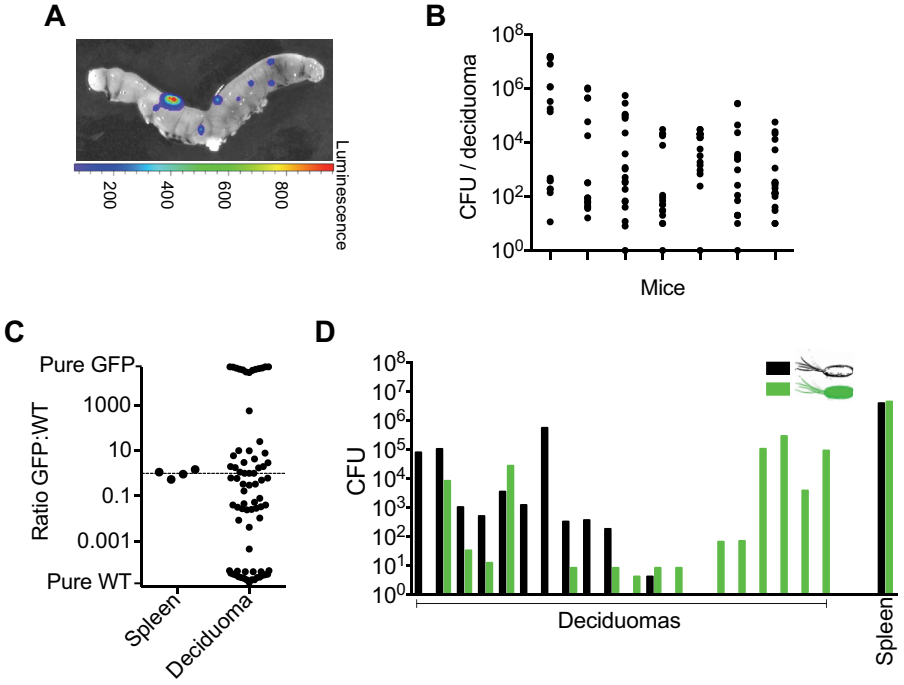

FIG 3 The decidua is a bottleneck *in vivo*. (A) Representative IVIS image of a decidualized uterus after intravenous infection with 2×10^6 CFU of bioluminescent *L. monocytogenes* strain 2C. (B) Deciduoma-bearing mice were infected intravenously with 4×10^5 CFU of wild-type (WT) *L. monocytogenes* on DPC6.5. The graph shows CFU in individual deciduomas 24 hpi. (C) Ratio of GFP-positive (GFP) to GFP-negative (wild-type) *L. monocytogenes* bacteria in spleen and individual deciduomas 24 h after intravenous infection with a 1:1 ratio of both strains. The horizontal dashed line indicates a ratio of 1. (D) GFP and WT *L. monocytogenes* CFU in individual deciduomas and spleen from one representative animal, prepared as described above for panel C.

bioluminescence imaging at 24 hpi revealed well-decidualized uteri with distinct foci of infection randomly distributed along the uterine horns (Fig. 3A). Next, we infected mice intravenously with 4×10^5 CFU of our laboratory wild-type *L. monocytogenes* strain 10403S. The bacterial burden in individual deciduomas was highly variable, with a range from 0 to 1.3×10^7 CFU at 24 hpi (Fig. 3B). The size of each deciduoma (measured in weight) and anatomic position within the uterine horns did not account for the observed variability in bacterial burdens (see Fig. S2 in the supplemental material). Importantly, a similar variability in the decidual bacterial burden was observed in pregnant mice intravenously injected on embryonic day 8.5 (E8.5) with green fluorescent protein (GFP)-expressing *L. monocytogenes*, which allowed us to use GFP positivity in live cells as a surrogate marker for intracellular infection. Consistent with a decidual barrier to initial bacterial seeding in the pregnant model, the frequency of GFP-positive (GFP^+) $CD45^+$ cells varied by a factor of 560-fold in deciduas from individual implantation sites (range, 0.02% to 11.2%) (Fig. S3).

To further characterize bacterial seeding of the decidua, we inoculated deciduoma-bearing mice with a 1:1 ratio of two wild-type *L. monocytogenes* strains that differed only in their abilities to express GFP. The total infectious dose was 4×10^5 CFU. As expected, the ratio of GFP-positive to GFP-negative *L. monocytogenes* bacteria in the spleen was 1.0, indicating that both wild-type strains colonized and grew equally well in the murine spleen. In contrast, the ratio between both strains was skewed in the deciduomas (Fig. 3C), indicating a low level of random seeding with few bacteria, i.e., a barrier to initial infection. Indeed, 35% of the deciduomas (26/74) contained a pure culture of either GFP-positive or GFP-negative organisms. Critically, however, these clonal cultures were observed in deciduomas with bacterial burdens as high as 1×10^6 organisms, suggesting that once colonized, the deciduas supported robust bacterial growth (Fig. 3D). Together, these results corroborated the findings in primary human

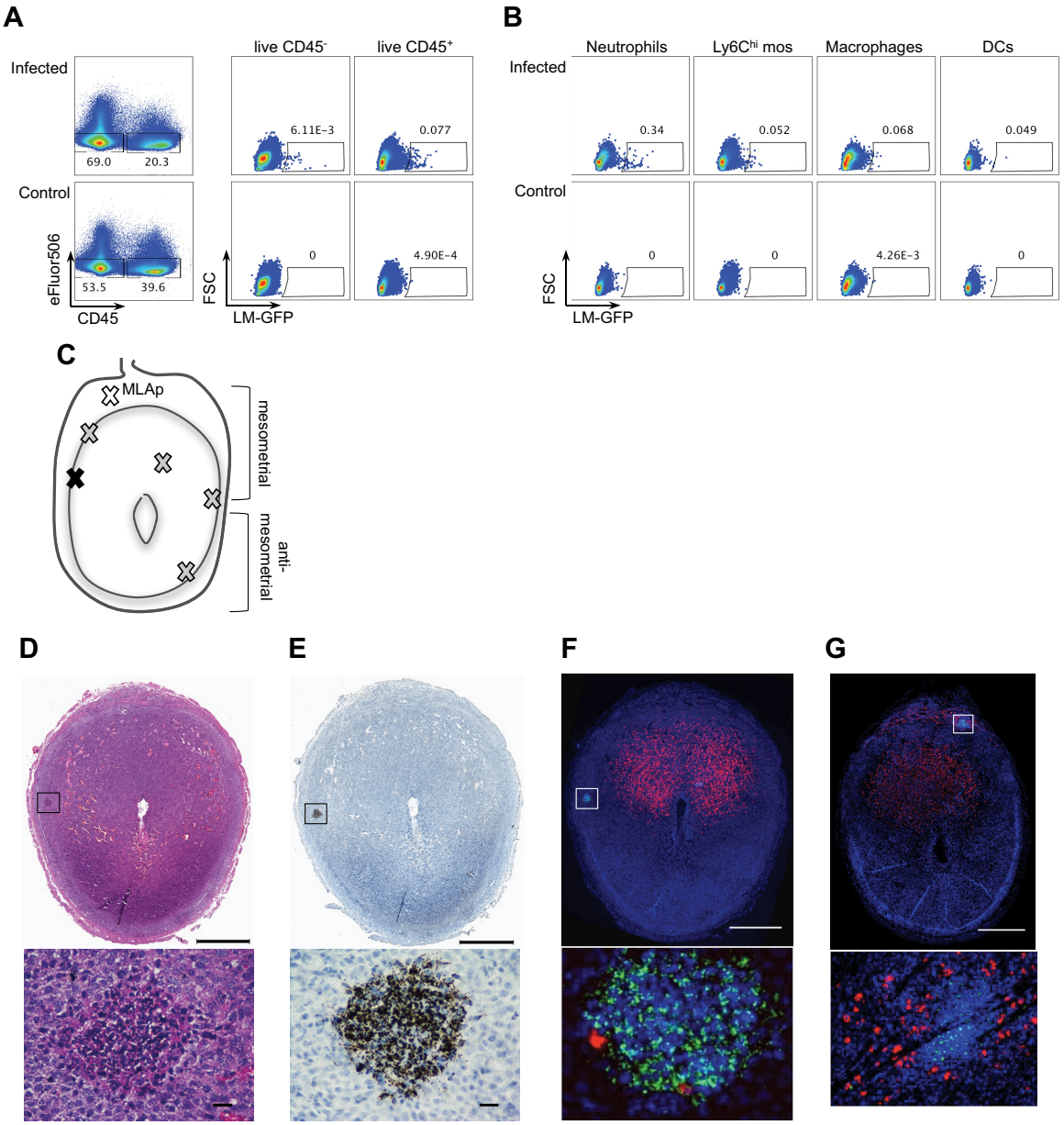

FIG 4 Uterine infection starts in discrete foci with infected CD45$^+$ and CD45$^-$ cells. (A and B) Deciduoma-bearing mice were infected intravenously with 1×10^6 GFP-expressing *L. monocytogenes* bacteria (LM-GFP) on DPC6.5. Infected cell populations were analyzed by flow cytometry at 24 hpi and compared to uninfected controls (for the gating strategy, see Fig. S4 in the supplemental material). (A) Percentages of live (Efluor506$^-$) CD45$^-$ and CD45$^+$ cells (left) and GFP$^+$ subsets (right). (B) Percentages of GFP$^+$ neutrophils, Ly6C^{hi} Mos, macrophages, and DCs. Shown are representative dot plots from 3 independent experiments. FSC, forward scatter. (C to G) Deciduoma-bearing mice were infected intravenously on DPC6.5 with 2×10^5 WT *L. monocytogenes* bacteria and analyzed at 24 hpi. (C) Cartoon depicting a decidualized uterus with the locations of all infectious foci (X). (D to G) Representative serial sections stained with H&E (D), anti-*L. monocytogenes* IHC (E), and immunofluorescence (F and G) with DBA-lectin (red), *L. monocytogenes* (green), and DAPI (blue). The bar in the low-power view is 1 mm. Rectangular boxes outline infectious foci that are displayed below at a higher magnification (bar, 25 μm).

decidual organ cultures and indicated that the decidua is difficult to infect but once the decidua is seeded, robust bacterial growth occurs.

***L. monocytogenes* infects both leukocytes and nonleukocytes in the decidua.** Next, we used flow cytometry to characterize early immune responses of the decidua following infection with GFP-expressing *L. monocytogenes*. GFP$^+$ cells were identified in the deciduas of three of five deciduoma-bearing infected mice (Fig. 4A); in contrast, no GFP$^+$ cells were detected in myometrial samples above the uninfected control background (data not shown). Decidual GFP$^+$ cells included CD45$^+$ leukocytes and a CD45$^-$

population, presumably comprised of decidual stromal cells, vascular endothelium, and/or glandular epithelium. The CD45$^+$ cells included neutrophils, Ly6C^{hi} Mos, macrophages, and DCs (Fig. 4B; see also Fig. S4 in the supplemental material). By frequency, the heaviest burden resided within neutrophils.

To enable histological analysis of infectious foci, we serially sectioned an entire uterus at 24 hpi. Histology revealed foci of Gram-positive, rod-shaped bacteria in 3 of 22 deciduomas: single foci were identified in 2 deciduomas, while 4 noncontiguous foci were uncovered in the third deciduoma. The locations of all infectious foci in the deciduoma-bearing uterus are schematized in Fig. 4C. Four foci were located adjacent to small vasculature at the decidual/myometrial border, one focus was detected in the mesometrial lymphoid aggregate of pregnancy (MLAp), and one focus was located in the stroma surrounding vascular channels in the mesometrial decidua. While statistical analysis could not be performed for the single uterus that was sectioned in its entirety, it is interesting to note that 4 of 6 foci were located at the decidual edge adjacent to the myometrium.

Visualized by H&E and IHC staining, foci contained a variable density of karyorrhectic debris, neutrophils, and *L. monocytogenes* bacteria (Fig. 4D and E). Immunofluorescence staining showed no change in the normal physiological distribution of cells that were stained with *Dolichos biflorus* agglutinin lectin (DBA-lectin) (Fig. 4F and G). Notably, one infectious focus was found in the MLAp among DBA-lectin$^+$ cells (Fig. 4G). Uterine NK cells did not form a ring around this infectious focus, and foci in other locations of the decidua or myometrial-decidual border were not surrounded by DBA-lectin$^+$ cells either, suggesting that NK cells do not migrate toward infectious foci. Consistent with previously reported findings (28), a robust mononuclear cell infiltrate in the decidua was not appreciated, and CD68$^+$ macrophages did not accumulate at foci of infection (Fig. S5).

Differential leukocyte dynamics in decidua versus myometrium. To gain insight into why the decidua is prone to robust growth of *L. monocytogenes*, we assessed changes in uterine leukocyte populations induced by infection. Previous studies showed that the decidua and myometrium differ significantly at baseline in regard to influx, migration, and blood-tissue partitioning of Mos, DCs, and lymphocytes (27, 34, 35). We thus characterized the tissue density of leukocyte subpopulations in the decidua versus the myometrium in response to infection of artificially decidualized mice.

Upon infection, we observed a significant reduction in the overall density of leukocytes (CD45$^+$ cells) within the decidua at 24 hpi (mean, 2.0×10^6 cells/mg in infected tissue versus 2.9×10^6 cells/mg in controls; $P < 0.05$) (Fig. 5A). This was mainly due to decreases in the densities of three cell types: Ly6C^{hi} Mos (mean, 5.4×10^5 cells/mg in infected tissue versus 1.0×10^6 cells/mg in controls; $P < 0.05$), B cells (mean, 3.7×10^4 cells/mg in infected tissue versus 1.4×10^5 cells/mg in controls; $P < 0.0005$), and macrophages (means, 7.9×10^4 cells/mg in infected tissue and 1.6×10^5 cells/mg in controls; $P < 0.05$). There was a small but insignificant increase in the decidual neutrophil density, and the decidual DC density did not change after infection. In contrast, in the myometrium, the overall density of CD45$^+$ cells did not significantly change after infection (Fig. 5B), but there was a reduction in the density of both subsets of DCs (for CD11b$^+$ DCs, mean of 2.5×10^4 cells/mg in infected tissue versus 4.1×10^4 cells/mg in controls; for CD11b$^-$ DCs, mean of 8.3×10^3 cells/mg in infected tissue versus 1.5×10^4 cells/mg in controls [both $P < 0.05$]), consistent with their migration to the draining lymph node. In contrast to the decidua, the density of Ly6C^{hi} Mos was increased in the myometrium (mean, 2.0×10^5 cells/mg in infected tissue versus 8.6×10^4 cells/mg in controls; $P < 0.05$).

To ascertain why these observed shifts in immune cell densities were tissue layer specific, we measured the levels of multiple chemokines semiquantitatively in decidual and myometrial tissue homogenates at 24 hpi (see Fig. S6 in the supplemental material). Most chemokines assayed were detected at higher levels in the myometrium

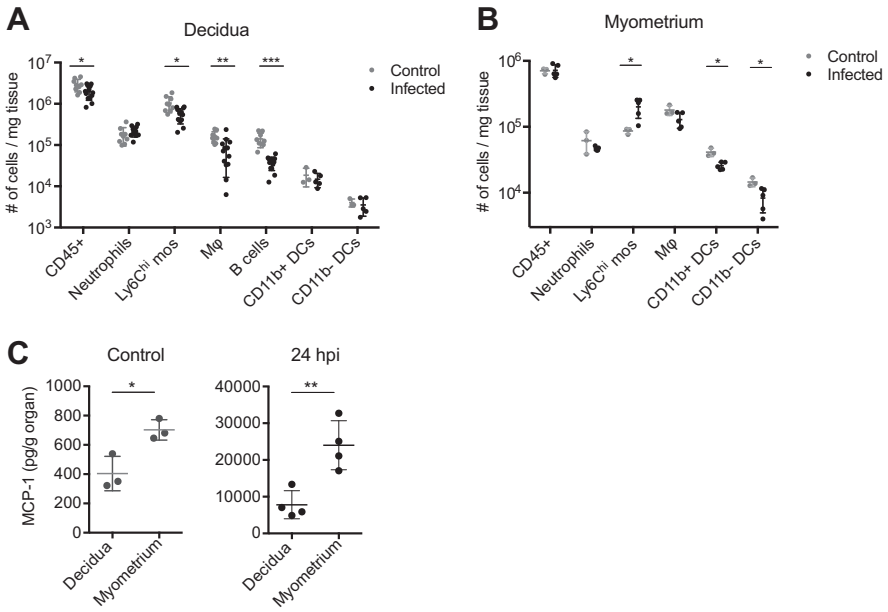

FIG 5 Decidual and myometrial leukocyte densities in response to infection. Deciduoma-bearing mice were infected intravenously with 4×10^5 wild-type *L. monocytogenes* bacteria on DPC6.5. (A and B) Leukocyte densities in the decidua and myometrium were determined by flow cytometry at 24 hpi and compared to the values for uninfected controls. (C) MCP-1 levels in the decidua and myometrium of infected (right) and uninfected control (left) mice. *, $P < 0.05$; **, $P < 0.005$; ***, $P < 0.0005$ (as determined by an unpaired *t* test with Welch correction). Data were obtained from at least 3 independent experiments. Mϕ, macrophage.

than in the decidua. Notably, those chemokines that showed greater increases in the myometrium than in the decidua included MCP-1, a CCR2 ligand known to be important for the recruitment of Ly6C^{hi} Mos. Additional quantitative measurements showed that MCP-1 levels were higher in the myometrium than in the decidua of both uninfected (702 versus 404 pg/g tissue; $P < 0.05$) and infected (23,996 versus 7,798 pg/g tissue; $P < 0.01$) tissues, translating into mean MCP-1 ratios of 1.8 in uninfected and 3.3 in infected myometrial versus decidual tissues (Fig. 5C). These MCP-1 gradients would be expected to favor a preferential influx of Ly6C^{hi} Mos into the myometrium.

DISCUSSION

The present study describes the dynamics of decidual infection by *L. monocytogenes*, a facultative intracellular bacterium that causes adverse pregnancy outcomes in women and serves as a model organism to study infection of the maternal-fetal interface. Surprisingly, we found that there is restricted bacterial colonization of both human and mouse deciduas. Our data suggest a model whereby high-titer infection of deciduomas in mice is derived from very few founding *L. monocytogenes* organisms (Fig. 3C), and based on this, we now hypothesize that there are host barriers to initial colonization of the decidua. Because hematogenous infection of the maternal-fetal interface begins by microbial seeding of the decidua (3–7), restricted colonization of the decidua may help to account for the bottleneck to infection previously identified when the entire uterus and placenta were viewed together as a unit (36). We also show that, once colonized, the decidua supports robust bacterial growth in association with significant impairments in innate cellular immunity. Limited colonization, coupled with rapid and robust bacterial growth once seeded, is expected to yield high variability in the bacterial burdens among individual deciduomas in artificially decidualized mice or implantation site deciduas in pregnant mice. Indeed, we observed a difference in the bacterial burden measured at 24 hpi of almost 6 orders of magnitude for individual deciduomas (Fig. 3B), and this is consistent with previous reports of *L. monocytogenes* (28) and *Brucella abortus* (37) decidual infections.

One possibility to explain the low initial colonization of the decidua is that decidual stromal and/or endothelial cells possess certain cell-autonomous defense mechanisms. This notion is supported by previous reports describing the detection of natural antimicrobials such as beta-defensins 1, 2, and 3 and Elafin in human decidual specimens (38, 39) and is furthermore consistent with the 10-fold decreased ability of *L. monocytogenes*, supplied as extracellular organisms, to infect primary human decidual organ cultures compared to endometrial organ cultures. However, as recently reviewed by Anders et al. (40), more studies are needed to delineate the decidual stromal cell response to organisms such as *L. monocytogenes* that cause placental infections. Intriguingly, we recently reported results from a genomic screen that yielded ~200 listerial genes important for infection of the maternal-fetal interface (41). These genes included a gene encoding a secreted listerial protein, internalin P, which strongly promotes virulence at the maternal-fetal interface. It is attractive to hypothesize that internalin P and perhaps some of the other identified genes are critical for decidual infection. Future studies might now be designed to compare the relative infectivities of different mouse tertiary tissues, such as decidua, lung, and kidney, and to test the hypothesis that different virulence factors may promote virulence in these different environments.

Alternatively, since experiments in pregnant guinea pigs suggested that *L. monocytogenes* traffics to the maternal-fetal interface inside infected cells, rather than as extracellular organisms (25), it is possible that the limited decidual seeding is also due to inefficient access to the relevant host cells from the blood. The obvious candidates are Ly6C^{hi} Mos, since these cells have been directly implicated in the spread of *L. monocytogenes* to the murine brain (42, 43) yet show remarkably low rates of extravasation into the murine decidua (27). In contrast, the myometrium of each implantation site not only actively recruits Ly6C^{hi} Mos under physiological conditions through a CCR2-dependent mechanism (27) but, as we demonstrate here, also shows increased recruitment during infection in parallel with an increased expression level of MCP-1. This chemokine is a key ligand for CCR2, which drives Ly6C^{hi} Mo recruitment to multiple organs under a variety of conditions, including recruitment to the spleen in the nonpregnant model of listeriosis (19). These findings are moreover consistent with previously reported observations that the myometrium contains many more macrophages than the decidua and that macrophages are an important source of MCP-1 in the pregnant uterus (27).

Provocatively, Ly6C^{hi} Mos are also critically important for host defense against *L. monocytogenes* in murine liver and spleen (18, 22). Ly6C^{hi} monocytes are recruited to the sites of infection, where they differentiate into Tip-DCs. Tip-DCs are the main source of TNF-α at these infected tissue sites (18), and this cytokine potently activates macrophage bactericidal activity (reviewed in reference 44) and synergizes with gamma interferon (IFN-γ) and interleukin-6 (IL-6) to induce a listericidal capacity in infected hepatocytes (45). Thus, the relatively low density of Ly6C^{hi} Mos within the decidual parenchyma at baseline could make the decidua particularly vulnerable to listerial growth once it becomes colonized. Furthermore, in contrast to the myometrium, Ly6C^{hi} Mo densities in the decidua were decreased after infection. This cellular loss might be explained by cell death or the release of endothelium-associated Mos back into the bloodstream. Thus, our *in vivo* results suggest a model where Ly6C^{hi} Mos could play divergent roles in the pathogenesis of listeriosis at the maternal-fetal interface: limited recruitment to the decidua might protect this tissue from colonization but, once infected, might leave it vulnerable to bacterial growth. We hypothesize that the increased recruitment of monocytes that could differentiate into Tip-DCs within the decidua might lead to a better control of decidual *L. monocytogenes* infection via indirect effects of TNF-α on decidual macrophages and perhaps decidual stromal cells as well as direct microbicidal activity via iNOS. Future investigations should examine the cytokine environment of the infected decidua, where, with the paucity of Ly6C^{hi} monocytes, we hypothesize that there is a relative deficiency of TNF-α. Additionally, more investigation is needed to examine the intracellular course of *L. monocytogenes*

decidual stromal cell infection and whether this is altered by the exposure of these cells to TNF-α, a cytokine to which they have documented responsiveness (35). Interestingly, Ly6C^{hi} recruitment is important for the containment of other microbes, including *Toxoplasma gondii* (46) and *Mycobacterium tuberculosis* (47), both of which can colonize the maternal-fetal interface via the hematogenous route, suggesting that our findings might also be relevant to other pregnancy-associated infections.

Similar to Ly6C^{hi} Mos, macrophage densities were also decreased within the infected mouse decidua, while microscopic analysis of primary human decidual organ cultures and the murine decidualized uterus revealed that macrophages did not accumulate around bacterial foci. It must be noted that we did not formally establish that decidual macrophages have the capacity to migrate within our cultures; however, others have observed decidual macrophage migration in similar first-trimester organ cocultures of decidua and placental villi (48). Furthermore, the impairments in macrophage migration within decidual tissue are in line with previous work by Redline and colleagues, who demonstrated that macrophages do not localize near infectious foci in the deciduas of artificially decidualized and pregnant mice (6, 23, 28). Those workers also suggested that macrophage migration and responses might be constrained by the unique composition of the decidual stromal extracellular matrix (29, 49), a property that predicts that deficits in macrophage immunity could render the decidua vulnerable to not just *L. monocytogenes* but also other pathogens. Intriguingly, over a century ago, Alfred S. Warthin made the prescient observation that despite the presence of an abundance of *Mycobacterium tuberculosis* bacteria in the deciduas of women suffering from tuberculosis, granulomas, the histological hallmark of tuberculosis in all other tissues, were not present in the deciduas (50). In contrast, granulomas were observed in placental villi. While these observations are consistent with an absence of functional Th1 cells in the human decidua, they also raise the possibility of impaired macrophage differentiation and migration.

We also examined decidual NK cell localization relative to infectious foci because early accumulation of NK cells occurs at splenic foci, where NK cell-derived IFN-γ is important for macrophage activation (51). Bacterial foci in the decidualized uterus showed no evidence of DBA-lectin^{+} cell accumulation. Since DBA-lectin reactivity specifically identifies only the majority population of decidual NK cells (52), we cannot rule out the possibility that there is an accumulation of a minor population of DBA-lectin-negative decidual NK cells (53) or peripheral NK cells. However, the lack of NK cell accumulation is consistent with previous work on NK cell-deficient IL-15$^{-/-}$ mice that strongly argued against a role for these cells in protection against uteroplacental listeriosis (54).

The findings of restricted initial access of *L. monocytogenes* to the decidua followed by unfettered bacterial proliferation without host immune control beautifully illustrate the competing demands imposed upon the decidua in its dual function in reproduction and host defense and are consistent with the various ways in which the decidua has attenuated the function of indwelling immune cells to minimize potential damage to the conceptus (27, 34, 35). Moreover, dividing the pathogenesis of decidual listeriosis into two phases may explain the key clinical features of its downstream outcome, placental listeriosis. Thus, while placental listeriosis is relatively rare, with recently reported incidence rates of 2.80 and 12.40 cases per 100,000 in non-Hispanic and Hispanic women, respectively (55), it generates significant neonatal morbidity and mortality often associated with the generation of large placental abscesses containing *L. monocytogenes* (56). This kind of two-tiered pattern is similar to what is seen with other pathogens that colonize the placenta via the maternal bloodstream, suggesting that the features of the decidua dissected here might be broadly relevant.

Importantly, the above-described view of decidual/placental listeriosis is able to explain the heightened susceptibility of pregnant women to *L. monocytogenes* infection without invoking a role for immune suppression at the systemic level. Previous studies considering the possibility that pregnancy may confer a systemic state of immunosuppression demonstrated that pregnant mice with reduced regulatory T (Treg) cell

numbers show not only improved bacterial clearance when infected with *L. monocytogenes* but also frequent abortion, although the mechanism of abortion is unclear (57, 58). Those studies, however, neither examined the bacterial burdens within the decidua and myometrium nor considered the possibility that pregnant mice are unable to clear *L. monocytogenes* because the infected decidua, insulated from the maternal immune system, might provide a source of organisms that perpetually seed the blood (25). Thus, Treg cell depletion during pregnancy might improve bacterial clearance not because it derepresses the maternal immune system but because it causes abortion through as-yet-defined mechanisms and thus removes the source of infection. This view is consistent with observations that pregnant women are not generally more susceptible to infection but rather are specifically susceptible to a select group of organisms that infect the maternal-fetal interface, including *L. monocytogenes* (59). This view is also consistent with observations that maternal vaccination is effective, if not enhanced, during gestation (60–62) and that $CD8^+$ T cell responses to viral antigens are not significantly diminished in pregnant versus nonpregnant mice (63). These considerations thus underscore the importance of further research into intrauterine mechanisms that promote or impede the colonization and growth of organisms that seed the maternal-fetal interface from the blood. Such studies might take advantage of manipulating *L. monocytogenes* virulence factors that render the organism capable of decidual infection.

MATERIALS AND METHODS

Ethics statement. This work was conducted according to Declaration of Helsinki principles. The use of human tissue was approved by the Institutional Review Board (IRB) (approval number 11-05530). All patients provided written informed consent for the collection of samples and subsequent analysis. Experiments with artificially decidualized mice were performed at the University of California—San Francisco (UCSF), and approved by the Institutional Animal Care and Use Committee (approval number AN101524-02) at UCSF. Experiments with pregnant mice were performed at NYU School of Medicine and approved by the NYU Institutional Animal Care and Use Committee.

Preparation of human organ cultures. Deidentified decidual specimens from elective terminations (gestational age, 6.0 to 14.3 weeks) were collected. Deidentified endometrial specimens from benign hysterectomies were freshly acquired from the UCSF-NIH Human Endometrial Tissue and DNA Bank (64). Briefly (see reference 65 for the complete protocol), 2-mm^3 fragments of decidua parietalis or endometrium were microdissected; placed onto Transwell filters (30-mm diameter, 0.4 μm, hydrophilic polytetrafluoroethylene [PTFE] membrane; Millipore) precoated with 0.1 ml Matrigel (BD Biosciences); and immediately cultured in Dulbecco modified Eagle medium (DMEM)–F-12 medium (1:1, vol/vol) with Gibco GlutaMAX (Thermo Fisher Scientific) supplemented with 2.5% fetal bovine serum, 100 IU/ml penicillin, 100 μg/ml streptomycin, 50 μg/ml gentamicin, and 1.25 μg/ml amphotericin B (Thermo Fisher Scientific). Explants were cultured at 37°C in 21% O_2 and 5% CO_2. Medium was changed every 24 to 48 h.

Bacterial strains. The wild-type *L. monocytogenes* strain was 10403S or 10403S expressing GFP (66, 67). Bioluminescent *L. monocytogenes* strain 2C, constructed by using the *lux-kan* hybrid transposon of plasmid pAUL-A Tn4001 *luxABCDE* Km^r as previously described (33), was kindly provided by Jonathan Hardy.

Infection of human organ cultures. Bacteria were cultured in brain heart infusion (BHI) broth (BD) at 30°C and washed three times with phosphate-buffered saline (PBS) prior to dilution. The intracellular growth and spread of *L. monocytogenes* were assayed as previously described (68), with the following minor modifications: at the indicated times after infection, organ cultures were removed and homogenized in 1 ml distilled water (dH_2O) supplemented with 0.1% Triton X-100 (Sigma-Aldrich) by using a Kimble-Chase Kontes pellet pestle (Sigma-Aldrich), and aliquots were plated on BHI agar (BD) and cultured at 37°C for the enumeration of CFU.

Mice. (i) Deciduoma induction. B6CBAF1/J females (aged 8 to 12 weeks; Jackson Laboratories) were used in all experiments because of the high fecundity of this strain. Females were mated to vasectomized ICR males (Taconic Farms) to initiate the hormonal state that supports decidualization. Mice were monitored daily for copulation plugs, and noon of that day was designated "day 0.5 postcopulation" or DPC0.5. This designation corresponds to the standard of days postconception but acknowledges that the mice do not actually become pregnant. Deciduomas were induced by intraluminal uterine infusion of 20 μl sterile sesame oil (Sigma-Aldrich) on DPC3.5 via a nonsurgical, transcervical approach detailed previously (34). After infection, daily subcutaneous injection of 2 mg progesterone (Sigma-Aldrich) was administered to maintain the decidua after the loss of ovarian function secondary to systemic inflammation (69).

(ii) Pregnant mice. Animals were purchased from Taconic Farms. All mating experiments used virgin B6CBAF1/J females and C57BL/6 males; noon of the day of the copulation plug was counted as E0.5.

(iii) Infection. Bacteria were cultured in BHI broth to exponential phase, and aliquots were frozen in BHI medium with 4% (vol/vol) glycerol and used within 1 year of freezing. On the day of infection, bacterial aliquots were thawed, rinsed three times, and diluted in sterile PBS to the indicated doses. Mice

were inoculated intravenously in a volume of 0.2 ml via the lateral tail vein. Deciduoma-bearing mice were infected on DPC6.5. When indicated, littermate control B6CBAF1/J females were infected in parallel. Pregnant mice were infected with 1×10^6 GFP-expressing *L. monocytogenes* bacteria on E8.5. The infectious dose was confirmed by serial dilution on BHI agar. Mice were sacrificed at the indicated times postinfection, and organs were harvested in a sterile fashion. For the determination of bacterial burden, organs were homogenized in sterile PBS with 0.05% Triton X-100 (Sigma-Aldrich) by using a T25 digital Ultra-Turrax instrument (IKA), and serial dilutions were plated onto BHI agar.

Cell preparation and flow cytometry for leukocyte density determination. For the determination of decidual and myometrial tissue densities by flow cytometry, the harvested uterine tissues were processed as previously described (34). Briefly, uteri were immediately placed into cold Ca^{2+}/Mg^{2+}-replete Hanks' balanced salt solution (HBSS), the decidua and myometrium were separated and weighed, and tissues were finely minced. Minced tissues were enzymatically digested at 37°C in Ca^{2+}/Mg^{2+}-replete HBSS with 0.28 Wunsch units of Liberase and 30 μg/ml DNase I (Roche) for 30 min with periodic mixing, rinsed in Ca^{2+}/Mg^{2+}-free PBS with 5 mM EDTA (Corning), and reincubated in the same manner with Ca^{2+}/Mg^{2+}-replete HBSS buffer and digestion enzymes. Samples were filtered through a 70-μm cell strainer, and red blood cells (RBCs) were lysed with RBC lysis buffer (eBioscience). Total viable cells were assessed manually on a hemocytometer with trypan blue exclusion. The density of each leukocyte subset was calculated as [(total cells) $\times$ (flow cytometric frequency)]/tissue weight in milligrams.

Prior to antigen-specific staining, cells were incubated in FcγR block (clone 2.4G2; BD Biosciences). Populations were subtyped by using fluorochrome-conjugated antibodies specific for murine major histocompatibility complex class II (MHC-II) (M5/114.15.12), CD45 (30-F11), CD19 (1D3), CD11b (M1/70), Ly6C (HK1.4), F4/80 (BM8; C1:A3-1), Gr-1 (RB6-8C5), and CD11c (N418), purchased from BD Biosciences, eBioscience, Tonbo Biosciences, or BioLegend. Dead cells were identified by 4′,6-diamidino-2-phenylindole (DAPI) (Affymetrix) or Fixable Dead Cell Viability Dye eFluor-506 (eBioscience) staining. Fluorescence compensation controls were prepared with an anti-rat and anti-hamster Ig,κ/Negative Control Compensation Particles set (BD Biosciences), and samples were acquired by using FACSDiva software on a BD Fortessa or LSRII machine (BD Biosciences) and analyzed by using FlowJo (Tree Star) or FCS Express (De Novo Software) software.

Bioluminescence imaging for bacterial localization. Uteri from deciduoma-bearing mice were harvested in cold PBS at 24 hpi with 2×10^6 *L. monocytogenes* strain 2C bacteria. Uteri from control deciduoma-bearing uninfected animals were harvested at DPC6.5 to DPC7.5. Organs were imaged on petri dishes in an IVIS (*in vivo* imaging system) Spectrum instrument (PerkinElmer) and with Living Image software, with an exposure time of 3 min, a binning factor of 8, and F-stop of f/1.

Immunohistochemistry. (i) Mouse. The uterus from a deciduoma-bearing mouse infected with 2×10^5 wild-type *L. monocytogenes* bacteria was harvested at 24 hpi and immediately fixed in fresh 10% neutral buffered formalin for 24 h. With a clean scalpel, the uterus was sliced between each deciduoma, generating 22 total deciduomas, which were processed and paraffin embedded according to standard techniques. Serial 5- to 7-μm sections were generated on a microtome and placed onto glass slides (2 to 3 sections per slide). Screening for bacterial foci was conducted by staining one in every five slides with either H&E or McDonald's Gram stain kit (American MasterTech), and slides were evaluated twice at high power by a pathologist (G.R.). We estimated that this should enable the detection of all infectious foci measuring at least 35 μm. The presence of rod-shaped organisms and/or focal hypercellularity defined suspected foci. These suspected foci were confirmed by immunohistochemistry on adjacent tissue sections using polyclonal rabbit *Listeria* O antiserum (BD Difco). Whole slides were imaged at a $\times$40 magnification on an Aperio ScanScope XT instrument (Leica Biosystems).

(ii) Human. At the indicated times postinfection, decidual organ cultures were rinsed three times in PBS and immediately fixed in fresh 10% neutral buffered formalin for 24 to 48 h. Tissue was processed and paraffin embedded, and serial 5-μm sections were generated. Immunohistochemistry was performed by using polyclonal rabbit *Listeria* O antiserum (BD Difco).

Immunofluorescence. (i) Mouse. Paraffin-embedded tissue sections from the mouse uterus described above were utilized for DBA-lectin and anti-CD68 immunostaining. For DBA-lectin staining, antigen retrieval was performed by incubating deparaffinized slides in IHC-Tek Epitope Retrieval solution (IHC World) for 40 min using an IHC-Tek Epitope Retrieval Steamer set. For CD68 staining, antigen retrieval was performed in citrate buffer (pH 6) at 110°C. For blocking, slides were incubated in Background Buster (Innovex Biosciences) or with donkey serum. For primary staining, biotinylated DBA-lectin (1:1,000; Vector Laboratories) or anti-CD68 (polyclonal rabbit, 1:2,000; LifeSpan BioSciences) and polyclonal rabbit *Listeria* O antiserum (1:500; BD Biosciences) were incubated overnight in PBS with 1% bovine serum albumin (BSA), 0.4% Triton X-100 (Sigma-Aldrich), and 5% normal goat or donkey serum (Jackson ImmunoResearch Laboratories) at 4°C. Secondary staining was performed with Alexa Fluor 568-streptavidin (1:200; ThermoFisher Scientific) or donkey anti-rabbit-horseradish peroxidase (HRP) (1:200; Jackson ImmunoResearch) with biotin-tyramide amplification, Alexa Fluor 594-streptavidin (1:200; Life Technologies), and Alexa Fluor 488 goat anti-rabbit (1:500; ThermoFisher Scientific). Nuclei were stained with DAPI (Affymetrix), and sections were mounted in Vectashield mounting medium (Vector Laboratories). Stitched images were acquired on a Nikon Ti-E epifluorescence microscope with a DS-Ri2 camera and NIS-Elements 4.30 software (Nikon) or with a Keyence BZ-X700 fluorescence microscope and BZ-X Analyzer software (Keyence).

(ii) Human. Paraffin-embedded tissue sections from the decidual organ cultures described above were utilized for anti-CD68 immunostaining. Antigen retrieval was performed by incubating deparaffinized slides in citrate buffer (pH 6) in a microwave pressure cooker for 12 min. Slides were blocked with goat serum, and primary staining was performed with anti-CD68 (mouse clone PGM1, 1:100; Agilent

Technologies) and polyclonal rabbit *Listeria* O antiserum, as described above. Secondary staining was performed with Alexa Fluor 488 goat anti-rabbit and Alexa Fluor 594 goat anti-mouse (1:200; ThermoFisher Scientific), nuclei were counterstained with DAPI, and sections were mounted in Vectashield. Stitched images were acquired with a Keyence BZ-X700 instrument.

Cytokine measurements. For cytokine analysis, organs were harvested in cold Ca^{2+}/Mg^{2+}-replete HBSS, and the decidua and myometrium were separated. Samples were henceforth maintained on ice during processing. Tissues were homogenized by using a T25 digital Ultra-Turrax instrument (IKA) in sterile PBS with a complete EDTA-free protease inhibitor cocktail (Roche) and centrifuged, and supernatants were frozen in 1% Triton X-100 (Sigma-Aldrich). The MCP-1 levels were measured with a BD Cytometric Bead Array (CBA) Mouse Inflammation kit (BD Biosciences). Samples were prepared according to the manufacturer's protocols, acquired by using FACSDiva software on a BD Fortessa or LSRII machine (BD Biosciences), and analyzed by using FlowJo (Tree Star), with best-fit standard curves generated by using PRISM software (version 6.0; GraphPad).

Chemokine measurements. For chemokine analysis, organs were harvested and homogenized as described above for cytokine analysis.

The protein concentration was determined with a Pierce bicinchoninic acid (BCA) protein assay kit (ThermoFisher Scientific). The relative levels of selected mouse chemokines in infected and uninfected decidual and myometrial tissue lysates were determined with a Proteome Profiler Mouse Chemokine Array kit (R&D Systems) according to the manufacturer's protocols. Pixel densities on developed X-ray film were scanned, analyzed with FIJI software to determine the average pixel density (signal) for each chemokine, and normalized to control spots.

Statistical analysis. Statistical tests (Student *t* test, analysis of variance [ANOVA] with repeated-measures and Dunnett's multiple-comparison tests, and Pearson *r*) were performed where indicated in the figure legends (PRISM software version 6.0; GraphPad). *P* values of ≤ 0.05 were considered significant.

SUPPLEMENTAL MATERIAL

Supplemental material for this article may be found at https://doi.org/10.1128/IAI.00153-17.

SUPPLEMENTAL FILE 1, PDF file, 2.2 MB.

ACKNOWLEDGMENTS

We are grateful to Miko Kapidzic for technical advice; Ethan Castro for technical assistance; and Cristina Faralla, Holly Morrison-Ross, and David Lowe for helpful discussions. We acknowledge Mark Weinstein and the San Francisco General Hospital Pathology Department for expert assistance with immunohistochemistry.

This work was supported by National Institutes of Health grant RO1AI084928 and Burroughs Wellcome Fund grant 41259 to A.I.B. and by National Institutes of Health grants RO1AI106745 and RO1AI062980 to A.E. G.R. was supported by Society for Pediatric Pathology Young Investigator Research grant F32AI10895 and a University of California Partnerships for Faculty Diversity President's postdoctoral fellowship. The funders had no role in study design, data collection and analysis, decision to publish, or preparation of the manuscript.

REFERENCES

1. Gellersen B, Brosens IA, Brosens JJ. 2007. Decidualization of the human endometrium: mechanisms, functions, and clinical perspectives. Semin Reprod Med 25:445–453. https://doi.org/10.1055/s-2007-991042.
2. Erlebacher A. 2013. Immunology of the maternal-fetal interface. Annu Rev Immunol 31:387–411. https://doi.org/10.1146/annurev-immunol-032712-100003.
3. Robbins JR, Skrzypczynska KM, Zeldovich VB, Kapidzic M, Bakardjiev AI. 2010. Placental syncytiotrophoblast constitutes a major barrier to vertical transmission of *Listeria monocytogenes*. PLoS Pathog 6:e1000732. https://doi.org/10.1371/journal.ppat.1000732.
4. Chattopadhyay A, Robinson N, Sandhu JK, Finlay BB, Sad S, Krishnan L. 2010. *Salmonella enterica* serovar Typhimurium-induced placental inflammation and not bacterial burden correlates with pathology and fatal maternal disease. Infect Immun 78:2292–2301. https://doi.org/10.1128/IAI.01186-09.
5. Robbins JR, Zeldovich VB, Poukchanski A, Boothroyd JC, Bakardjiev AI. 2012. Tissue barriers of the human placenta to infection with *Toxoplasma gondii*. Infect Immun 80:418–428. https://doi.org/10.1128/IAI.05899-11.
6. Redline RW, Lu CY. 1988. Specific defects in the anti-listerial immune response in discrete regions of the murine uterus and placenta account for susceptibility to infection. J Immunol 140:3947–3955.
7. Weisblum Y, Panet A, Zakay-Rones Z, Haimov-Kochman R, Goldman-Wohl D, Ariel I, Falk H, Natanson-Yaron S, Goldberg MD, Gilad R, Lurain NS, Greenfield C, Yagel S, Wolf DG. 2011. Modeling of human cytomegalovirus maternal-fetal transmission in a novel decidual organ culture. J Virol 85:13204–13213. https://doi.org/10.1128/JVI.05749-11.
8. Posfay-Barbe KM, Wald ER. 2009. Listeriosis. Semin Fetal Neonatal Med 14:228–233. https://doi.org/10.1016/j.siny.2009.01.006.
9. Lamont RF, Sobel J, Mazaki-Tovi S, Kusanovic JP, Vaisbuch E, Kim SK, Uldbjerg N, Romero R. 2011. Listeriosis in human pregnancy: a systematic review. J Perinat Med 39:227–236. https://doi.org/10.1515/jpm.2011.035.
10. Unanue ER, Carrero JA. 2012. Studies with *Listeria monocytogenes* lead the way. Adv Immunol 113:1–5. https://doi.org/10.1016/B978-0-12-394590-7.00009-9.
11. Dussurget O, Bierne H, Cossart P. 2014. The bacterial pathogen *Listeria monocytogenes* and the interferon family: type I, type II and type III interferons. Front Cell Infect Microbiol 4:50. https://doi.org/10.3389/fcimb.2014.00050.
12. Conlan JW, North RJ. 1992. Early pathogenesis of infection in the liver with the facultative intracellular bacteria *Listeria monocytogenes*, *Francisella tularensis*, and *Salmonella typhimurium* involves lysis of infected hepatocytes by leukocytes. Infect Immun 60:5164–5171.

13. Conlan JW, North RJ. 1994. Neutrophils are essential for early anti-*Listeria* defense in the liver, but not in the spleen or peritoneal cavity, as revealed by a granulocyte-depleting monoclonal antibody. J Exp Med 179:259–268. https://doi.org/10.1084/jem.179.1.259.
14. Rosen H, Gordon S, North RJ. 1989. Exacerbation of murine listeriosis by a monoclonal antibody specific for the type 3 complement receptor of myelomonocytic cells. Absence of monocytes at infective foci allows *Listeria* to multiply in nonphagocytic cells. J Exp Med 170:27–37. https://doi.org/10.1084/jem.170.1.27.
15. Edelson BT, Bradstreet TR, Hildner K, Carrero JA, Frederick KE, KC W, Belizaire R, Aoshi T, Schreiber RD, Miller MJ, Murphy TL, Unanue ER, Murphy KM. 2011. CD8alpha(+) dendritic cells are an obligate cellular entry point for productive infection by *Listeria monocytogenes*. Immunity 35:236–248. https://doi.org/10.1016/j.immuni.2011.06.012.
16. Waite JC, Leiner I, Lauer P, Rae CS, Barbet G, Zheng H, Portnoy DA, Pamer EG, Dustin ML. 2011. Dynamic imaging of the effector immune response to *Listeria* infection in vivo. PLoS Pathog 7:e1001326. https://doi.org/10.1371/journal.ppat.1001326.
17. Shiloh MU, MacMicking JD, Nicholson S, Brause JE, Potter S, Marino M, Fang F, Dinauer M, Nathan C. 1999. Phenotype of mice and macrophages deficient in both phagocyte oxidase and inducible nitric oxide synthase. Immunity 10:29–38. https://doi.org/10.1016/S1074-7613(00)80004-7.
18. Serbina NV, Salazar-Mather TP, Biron CA, Kuziel WA, Pamer EG. 2003. TNF/iNOS-producing dendritic cells mediate innate immune defense against bacterial infection. Immunity 19:59–70. https://doi.org/10.1016/S1074-7613(03)00171-7.
19. Jia T, Serbina NV, Brandl K, Zhong MX, Leiner IM, Charo IF, Pamer EG. 2008. Additive roles for MCP-1 and MCP-3 in CCR2-mediated recruitment of inflammatory monocytes during *Listeria monocytogenes* infection. J Immunol 180:6846–6853. https://doi.org/10.4049/jimmunol.180.10.6846.
20. Serbina NV, Pamer EG. 2006. Monocyte emigration from bone marrow during bacterial infection requires signals mediated by chemokine receptor CCR2. Nat Immunol 7:311–317. https://doi.org/10.1038/ni1309.
21. Serbina NV, Kuziel W, Flavell R, Akira S, Rollins B, Pamer EG. 2003. Sequential MyD88-independent and -dependent activation of innate immune responses to intracellular bacterial infection. Immunity 19:891–901. https://doi.org/10.1016/S1074-7613(03)00330-3.
22. Kurihara T, Warr G, Loy J, Bravo R. 1997. Defects in macrophage recruitment and host defense in mice lacking the CCR2 chemokine receptor. J Exp Med 186:1757–1762. https://doi.org/10.1084/jem.186.10.1757.
23. Redline RW, Lu CY. 1987. Role of local immunosuppression in murine fetoplacental listeriosis. J Clin Invest 79:1234–1241. https://doi.org/10.1172/JCI112942.
24. Qiu X, Zhu L, Pollard JW. 2009. Colony-stimulating factor-1-dependent macrophage functions regulate the maternal decidua immune responses against *Listeria monocytogenes* infections during early gestation in mice. Infect Immun 77:85–97. https://doi.org/10.1128/IAI.01022-08.
25. Bakardjiev AI, Theriot JA, Portnoy DA. 2006. *Listeria monocytogenes* traffics from maternal organs to the placenta and back. PLoS Pathog 2:e66. https://doi.org/10.1371/journal.ppat.0020066.
26. Kruse A, Merchant MJ, Hallmann R, Butcher EC. 1999. Evidence of specialized leukocyte-vascular homing interactions at the maternal/fetal interface. Eur J Immunol 29:1116–1126.
27. Tagliani E, Shi C, Nancy P, Tay CS, Pamer EG, Erlebacher A. 2011. Coordinate regulation of tissue macrophage and dendritic cell population dynamics by CSF-1. J Exp Med 208:1901–1916. https://doi.org/10.1084/jem.20110866.
28. Redline RW, Shea CM, Papaioannou VE, Lu CY. 1988. Defective antilisterial responses in deciduoma of pseudopregnant mice. Am J Pathol 133:485–497.
29. Redline RW, McKay DB, Vazquez MA, Papaioannou VE, Lu CY. 1990. Macrophage functions are regulated by the substratum of murine decidual stromal cells. J Clin Invest 85:1951–1958. https://doi.org/10.1172/JCI114658.
30. Bany BM. 2014. Genome-wide analysis of the mouse deciduoma, p 297–308. *In* Croy BA, Yamada AT, DeMayo FJ, Adamson SL (ed), The guide to investigation of mouse pregnancy. Elsevier Inc, San Diego, CA.
31. Madjerek ZS. 1967. Comparison of the traumatic deciduoma with the normal decidual reaction in mice. Acta Physiol Pharmacol Neerl 14:520.
32. McConaha ME, Eckstrum K, An J, Steinle JJ, Bany BM. 2011. Microarray assessment of the influence of the conceptus on gene expression in the mouse uterus during decidualization. Reproduction 141:511–527. https://doi.org/10.1530/REP-10-0358.
33. Hardy J, Francis KP, DeBoer M, Chu P, Gibbs K, Contag CH. 2004. Extracellular replication of *Listeria monocytogenes* in the murine gall bladder. Science 303:851–853. https://doi.org/10.1126/science.1092712.
34. Collins MK, Tay CS, Erlebacher A. 2009. Dendritic cell entrapment within the pregnant uterus inhibits immune surveillance of the maternal/fetal interface in mice. J Clin Invest 119:2062–2073. https://doi.org/10.1172/JCI38714.
35. Nancy P, Tagliani E, Tay CS, Asp P, Levy DE, Erlebacher A. 2012. Chemokine gene silencing in decidual stromal cells limits T cell access to the maternal-fetal interface. Science 336:1317–1321. https://doi.org/10.1126/science.1220030.
36. Bakardjiev AI, Stacy BA, Portnoy DA. 2005. Growth of *Listeria monocytogenes* in the guinea pig placenta and role of cell-to-cell spread in fetal infection. J Infect Dis 191:1889–1897. https://doi.org/10.1086/430090.
37. Bosseray N. 1980. Colonization of mouse placentas by *Brucella abortus* inoculated during pregnancy. Br J Exp Pathol 61:361–368.
38. King AE, Kelly RW, Sallenave JM, Bocking AD, Challis JR. 2007. Innate immune defences in the human uterus during pregnancy. Placenta 28:1099–1106. https://doi.org/10.1016/j.placenta.2007.06.002.
39. King AE, Paltoo A, Kelly RW, Sallenave JM, Bocking AD, Challis JR. 2007. Expression of natural antimicrobials by human placenta and fetal membranes. Placenta 28:161–169. https://doi.org/10.1016/j.placenta.2006.01.006.
40. Anders AP, Gaddy JA, Doster RS, Aronoff DM. 3 January 2017. Current concepts in maternal-fetal immunology: recognition and response to microbial pathogens by decidual stromal cells. Am J Reprod Immunol. https://doi.org/10.1111/aji.12623.
41. Faralla C, Rizzuto GA, Lowe DE, Kim B, Cooke C, Shiow LR, Bakardjiev AI. 2016. InlP, a new virulence factor with strong placental tropism. Infect Immun 84:3584–3596. https://doi.org/10.1128/IAI.00625-16.
42. Drevets DA, Jelinek TA, Freitag NE. 2001. *Listeria monocytogenes*-infected phagocytes can initiate central nervous system infection in mice. Infect Immun 69:1344–1350. https://doi.org/10.1128/IAI.69.3.1344-1350.2001.
43. Drevets DA, Dillon MJ, Schawang JS, Van Rooijen N, Ehrchen J, Sunderkotter C, Leenen PJ. 2004. The Ly-6Chigh monocyte subpopulation transports *Listeria monocytogenes* into the brain during systemic infection of mice. J Immunol 172:4418–4424. https://doi.org/10.4049/jimmunol.172.7.4418.
44. Shaughnessy LM, Swanson JA. 2007. The role of the activated macrophage in clearing *Listeria monocytogenes* infection. Front Biosci 12:2683–2692. https://doi.org/10.2741/2264.
45. Szalay G, Hess J, Kaufmann SH. 1995. Restricted replication of *Listeria monocytogenes* in a gamma interferon-activated murine hepatocyte line. Infect Immun 63:3187–3195.
46. Robben PM, LaRegina M, Kuziel WA, Sibley LD. 2005. Recruitment of Gr-1+ monocytes is essential for control of acute toxoplasmosis. J Exp Med 201:1761–1769. https://doi.org/10.1084/jem.20050054.
47. Peters W, Scott HM, Chambers HF, Flynn JL, Charo IF, Ernst JD. 2001. Chemokine receptor 2 serves an early and essential role in resistance to *Mycobacterium tuberculosis*. Proc Natl Acad Sci U S A 98:7958–7963. https://doi.org/10.1073/pnas.131207398.
48. Hazan AD, Smith SD, Jones RL, Whittle W, Lye SJ, Dunk CE. 2010. Vascular-leukocyte interactions: mechanisms of human decidual spiral artery remodeling in vitro. Am J Pathol 177:1017–1030. https://doi.org/10.2353/ajpath.2010.091105.
49. McKay DB, Vazquez MA, Redline RW, Lu CY. 1992. Macrophage functions are regulated by murine decidual and tumor extracellular matrices. J Clin Invest 89:134–142. https://doi.org/10.1172/JCI115553.
50. Warthin AS. 1907. Tuberculosis of the placenta: a histological study with especial reference to the nature of the earliest lesions produced by the tubercle bacillus. J Infect Dis 4:347–368. https://doi.org/10.1093/infdis/4.3.347.
51. Kang SJ, Liang HE, Reizis B, Locksley RM. 2008. Regulation of hierarchical clustering and activation of innate immune cells by dendritic cells. Immunity 29:819–833. https://doi.org/10.1016/j.immuni.2008.09.017.
52. Zhang JH, Yamada AT, Croy BA. 2009. DBA-lectin reactivity defines natural killer cells that have homed to mouse decidua. Placenta 30:968–973. https://doi.org/10.1016/j.placenta.2009.08.011.
53. Chen Z, Zhang J, Hatta K, Lima PD, Yadi H, Colucci F, Yamada AT, Croy BA. 2012. DBA-lectin reactivity defines mouse uterine natural killer cell subsets with biased gene expression. Biol Reprod 87:81. https://doi.org/10.1093/biolreprod/87.s1.81.

54. Barber EM, Pollard JW. 2003. The uterine NK cell population requires IL-15 but these cells are not required for pregnancy nor the resolution of a *Listeria monocytogenes* infection. J Immunol 171:37–46. https://doi.org/10.4049/jimmunol.171.1.37.
55. Silk BJ, Date KA, Jackson KA, Pouillot R, Holt KG, Graves LM, Ong KL, Hurd S, Meyer R, Marcus R, Shiferaw B, Norton DM, Medus C, Zansky SM, Cronquist AB, Henao OL, Jones TF, Vugia DJ, Farley MM, Mahon BE. 2012. Invasive listeriosis in the Foodborne Diseases Active Surveillance Network (FoodNet), 2004-2009: further targeted prevention needed for higher-risk groups. Clin Infect Dis 54(Suppl 5):S396–S404. https://doi.org/10.1093/cid/cis268.
56. Benirschke K, Kaufmann P. 1995. Pathology of the human placenta, 3rd ed. Springer-Verlag, New York, NY.
57. Rowe JH, Ertelt JM, Aguilera MN, Farrar MA, Way SS. 2011. Foxp3(+) regulatory T cell expansion required for sustaining pregnancy compromises host defense against prenatal bacterial pathogens. Cell Host Microbe 10:54–64. https://doi.org/10.1016/j.chom.2011.06.005.
58. Rowe JH, Ertelt JM, Xin L, Way SS. 2012. *Listeria monocytogenes* cytoplasmic entry induces fetal wastage by disrupting maternal Foxp3+ regulatory T cell-sustained fetal tolerance. PLoS Pathog 8:e1002873. https://doi.org/10.1371/journal.ppat.1002873.
59. Robbins JR, Bakardjiev AI. 2012. Pathogens and the placental fortress. Curr Opin Microbiol 15:36–43. https://doi.org/10.1016/j.mib.2011.11.006.
60. Munoz FM, Ferrieri P. 2013. Group B *Streptococcus* vaccination in pregnancy: moving toward a global maternal immunization program. Vaccine 31(Suppl 4):D46–D51. https://doi.org/10.1016/j.vaccine.2012.11.026.
61. Zaman K, Roy E, Arifeen SE, Rahman M, Raqib R, Wilson E, Omer SB, Shahid NS, Breiman RF, Steinhoff MC. 2008. Effectiveness of maternal influenza immunization in mothers and infants. N Engl J Med 359:1555–1564. https://doi.org/10.1056/NEJMoa0708630.
62. Kay AW, Fukuyama J, Aziz N, Dekker CL, Mackey S, Swan GE, Davis MM, Holmes S, Blish CA. 2014. Enhanced natural killer-cell and T-cell responses to influenza A virus during pregnancy. Proc Natl Acad Sci U S A 111:14506–14511. https://doi.org/10.1073/pnas.1416569111.
63. Constantin CM, Masopust D, Gourley T, Grayson J, Strickland OL, Ahmed R, Bonney EA. 2007. Normal establishment of virus-specific memory CD8 T cell pool following primary infection during pregnancy. J Immunol 179:4383–4389. https://doi.org/10.4049/jimmunol.179.7.4383.
64. Sheldon E, Vo KC, McIntire RA, Aghajanova L, Zelenko Z, Irwin JC, Giudice LC. 2011. Biobanking human endometrial tissue and blood specimens: standard operating procedure and importance to reproductive biology research and diagnostic development. Fertil Steril 95:2120–2122. https://doi.org/10.1016/j.fertnstert.2011.01.164.
65. Rizzuto GA, Kapidzic M, Gormley M, Bakardjiev AI. 21 July 2016. Human placental and decidual organ cultures to study infections at the maternal-fetal interface. J Vis Exp https://doi.org/10.3791/54237.
66. Bishop DK, Hinrichs DJ. 1987. Adoptive transfer of immunity to *Listeria monocytogenes*. The influence of in vitro stimulation on lymphocyte subset requirements. J Immunol 139:2005–2009.
67. Shen A, Higgins DE. 2005. The 5′ untranslated region-mediated enhancement of intracellular listeriolysin O production is required for *Listeria monocytogenes* pathogenicity. Mol Microbiol 57:1460–1473. https://doi.org/10.1111/j.1365-2958.2005.04780.x.
68. Jones S, Portnoy DA. 1994. Intracellular growth of bacteria. Methods Enzymol 236:463–467. https://doi.org/10.1016/0076-6879(94)36034-0.
69. Erlebacher A, Zhang D, Parlow AF, Glimcher LH. 2004. Ovarian insufficiency and early pregnancy loss induced by activation of the innate immune system. J Clin Invest 114:39–48. https://doi.org/10.1172/JCI200420645.